Acta Mineralogica-Petrographica, Szeged, XXXVI, 17–33, 1995

CRYSTALLIZATION OF AMPHIBOLES IN THE KID VOLCANIC COMPLEX, SOUTHERN SINAI, EGYPT: IMPLICATIONS FOR MAGMA EVOLUTION

I. KUBOVICS* and A. M. ABDEL-KARIM**

*Department of Petrology and Geochemistry, Eötvös University
and **Geology Department, Zagazig University

ABSTRACT

The Kid volcanics consist of three main suites namely, basaltic andesite-andesite (BA-A), trachydacite-dacite (TD-D) and rhyodacite-alkali rhyolite (RD-AR). Microprobe analyses of phenocrysts and groundmass of the amphiboles from rocks of these volcanic suites are presented in this paper. Amphiboles from BA-A suite range from tschermakite phenocryst cores to ferro tschermakitic hornblende phenocryst rims and groundmass. TD-D suite has ferroan pargasite phenocrysts and ferroan pargasitic hornblende groundmass. Amphiboles from RD-AR suite range from kaersutite and ferroan pargasite phenocryst cores to magnesian hastingsitic hornblende phenocryst rims and magnesian hastingsite groundmass.

The amphiboles of Kid volcanics are Ti-rich, calcic-type. In most cases, amphibole phenocrysts from BA-A and RD-AR suites have the same evolution, reflect their cognate magmas. Moreover, both the TD-D and RD-AR suites have close genetic relationship. The progressive evolutionary trend from phenocryst cores to phenocryst rims and groundmass and from intermediate (BA-A) to felsic (RD-AR) suite are responsible for the magmatic evolution of the Kid volcanic suites. In contrast, the concentration of amphibole composition as a function of pressure and temperature suggest an opposite trend for the grade of metamorphism of these suites. These calcic amphiboles are expected to be formed at high temperature (~700–1000 °C) and low pressure (~0.2–3 Kb.) conditions.

INTRODUCTION

Amphibole represents the dominant mafic mineral phase in many rocks of intermediate and felsic compositions. Due to its importance, a large body of miscellaneous work on amphibole is scattered throught the scientific literature. More recently, amphibole in intermediate and felsic compositions has been thoroughly studied by several investigators including LEAKE (1978), CAMERON and PAPIKE (1979), WONES and GILBERT (1981), HAWTHORNE (1983), SCHULZ-KUHNT et al. (1990).

Generally, the Precambrian volcanic rocks in the Egyptian basement belong to the three major geotectonic units (RIES et al., 1983 and EL-GABY et al., 1988); namely, the lower unit comprises low-K tholeiitic basalts which are integral part of an ophiolite association. The second unit belongs to the island arc association of andesite, dacite and volcanoclastics with subordinate basalt overthrusted on the former unit (EL-GABY et al., 1988), and the third unit manifested by a vast subaerial, calc-alkaline volcanics (Dokhan-type) rhyolites and rhyodacites are dominant rock types of this unit.

* H–1088 Budapest, Múzeum krt. 4/A
** Zagazig, Egypt

Amphibole is represent in diverse varieties in many volcanics of the Kid segment of southeastern Sinai (*Fig. 1.*). In this study, a number of fresh amphibole samples have been analyzed to enable us to examine the mineralogical variations with each volcanic unit and, to examine the compositional zoning of individual amphibole grains. The purpose of this work is: 1. to study the amphibole chemistry using new microprobe analytical data, 2. to illustrate the compositional trends, crystallization history and evolution of the amphibole of the various rocks, and 3. to discuss the role of amphibole on magma evolution.

GENERAL GEOLOGY

The Kid supracrustal segment, southeastern Sinai (*Fig. 1.*), is largely occupied by a volcano-sedimentary succession intruded by a number of igneous intrustions including layered gabbro, quartz monzodiorite, G2 and G3 younger granites and minor albitite (EL-GABY et al., 1991). The succession is overprinted by a low-pressure metamorphism (REYMER et al., 1984). It lies unconformably above partially migmatized gneisses.

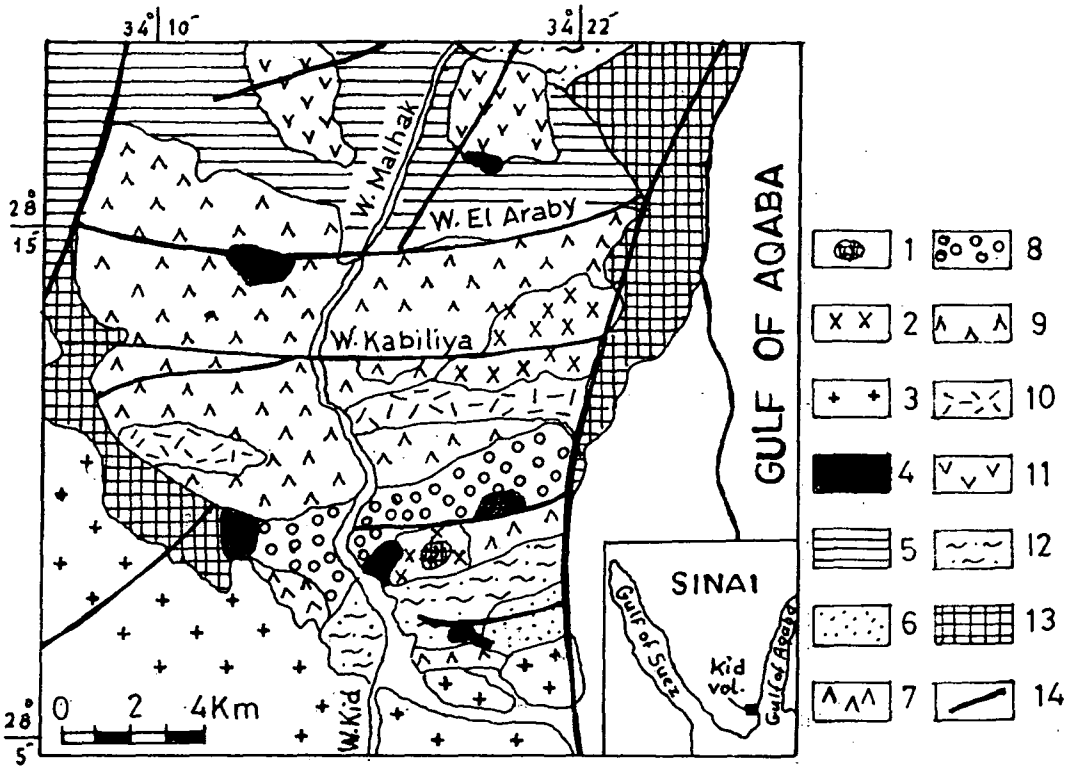

Fig. 1. Geologic map of the Kid volcanics (after HASSANEN, 1992).
1 = albitite; 2 = younger granite; 3 = gneissose granite; 4 = Upper Volcanic Sequence (basaltic rocks); 5 = Hammamate clastic sediments; Middle Volcanic Sequence [upper unit (6 = high K-dacite with pyroclastics, 7 = alkali rhyolite), 8 = Kid metaconglomerate, lower unit (9 = rhyolite and dacite with pyroclastics, 10 = andesite)]; 11 = Lower Volcanic Sequence (metabasalt and metabasaltic andesite); 12 = marine sediments, 13 = gneissose diorite, gneiss and amphibolite, 14 = fault lines.

The geology and geochemistry of the Kid volcanics have been discussed elsewhere (SHIMRON, 1984; GHONEIM et al., 1985; EL-GABY et al., 1991; HASSANEN, 1992). Nevertheless, the magmatic evolution of these rocks is still a matter of great dispute. This work represents the first mineralogical study in the Wadi Kid area. The following is a synopsis of the geology of the volcanics in question.

The main volcanic components of the Kid volcanics are lava flows, sheets, subvolcanics and pyroclastics of a wide composition range from basalt to rhyolite. The associated sedimentary rocks vary in lithology and deposition including metagreywackes, metaconglomerates, epiclastics, mudstone and turbidites. The Kid volcanics can be subdivided into three main volcanic sequences. These are: lower, middle and upper volcanic sequences.

The lower volcanic sequence consists of slightly to moderately metamorphosed intermediate and minor mafic volcanics. The rocks of this sequence occur as sheets, flows and sills. The middle sequence, on the other hand, are fresh and weakly metamorphosed, and occured as subvolcanic dyke-like intrusions and sheets intruded into the former volcanic unit. The rocks of this unit comprises felsic and minor intermediate volcanics. The middle sequence is separated into two stratigraphic units by thick beds of Kid metaconglomerate belonging to Hammamate clastic type sediments. The lower unit is dominated by rhyolite and less common andesite and their pyroclastic equivalents. The upper unit consists mainly of felsic volcanics and pyroclastics. HASSANEN (1992) added a new sequence (e. g., upper volcanic sequence) to Kid volcanics. This sequence is locally distributed and comprises mafic and intermediate alkaline volcanics and is separated from the middle sequence by Hammamate clastic sediments. Most of these volcanic sequences are cut by doleritic dykes. The intermediate rocks of the lower sequence and the felsic rocks of middle volcanic sequences which constitute the main volcanic rocks are the amphibole bearing volcanic suites of the region, and are the subject of this mineralogical study.

PETROGRAPHY

The lower volcanic unit is variably metamorphosed aphyric to phyric basaltic andesite, andesite, trachydacite and dacite. The pyroclastics comprise ignimberite, tuffs and agglomerate of the same compositions. The middle volcanic unit, on the other hand, is unmetamorphosed aphyric and phyric rhyolite and less abundant rhyodacite and their compositionally equivalent tuffs and lava flows. Detailed petrographic description is given by EL-GABY et al. (1991) and HASSANEN (1992).

The following account summarizes the main petrographic features of the amphibole-bearing volcanic rocks in question.

a) Basaltic andesite-andesite (BA-A) suite constitutes the main components of the lower volcanic unit. They are fine grained, commonly porphyritic greyish green in colour. Intergranular and porphyritic textures are the most common rock textures. They are composed of plagioclase (An_{40-50}) and amphibole phenocrysts embedded in pilotaxitic groundmass composed of the same minerals and subordinate Fe-oxides and apatite. Augite is present in some rock samples. Secondary metamorphic products include epidote, chlorite and sphene. Amphibole occurs as pale green-brown prismatic phenocrysts (0.4–1.9 mm long) and as anhedral crystals in the groundmass. It is occasionally zoned (*Fig. 2*). Zoned phenocrysts exhibit pleochroic pale green to deep brown-green colour outer rims, and blueish green colour outermost rims. Chlorite, epidote and Fe-oxide are the main alteration products of the amphibole.

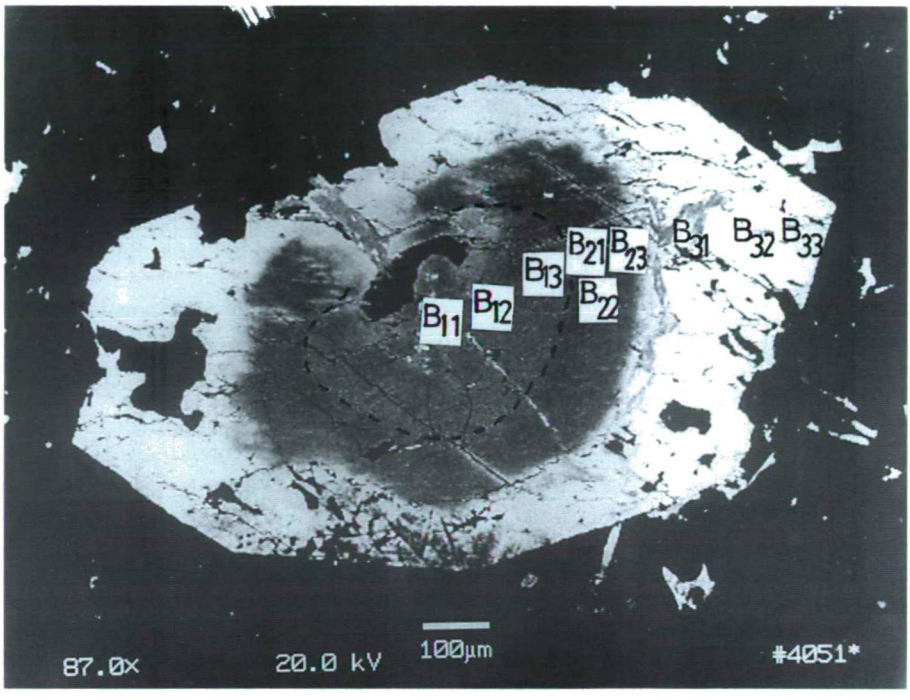

Fig. 2. Photomicrograph of a zoned phenocryst from basaltic andesite-andesite (BA-A) suite showing tschermakite inner and outer cores and ferro tschermakitic hornblende rim.
B_{11}, B_{12}, ... = Locations of analyses

b) Trachydacite-dacite (TD-D) suite is recorded in the lower unit of the middle volcanic sequence are fine grained, light green, yellowish green or grey and frequently porphyritic. They consist of phenocrysts of plagioclase (An_{30-44}) and less abundant amphibole, disposed in a fine grained flow banding and trchytoid groundmass composed of the same composition and potash feldspar, quartz and biotite and subordinate Fe-oxides, sphene and apatite. Amphibole occurs as idiomorphic prismatic and rhombic-shape phenocrysts (0.3–1.8 mm long) or as subhedral crystals in the groundmass. It is relatively homogeneous in colour (mainly yellow to brown tint), and does not show compositional zoning (*Fig. 3*). Amphibole crystals occasionally rimmed by thick alteration margin composed of uralite, chlorite and Fe-oxides, are recorded.

c) Rhyodacite-alkali rhyolite (RD-AR) suite is the dominant rock types in the upper unit of middle volcanic sequence. These two rock types are fine grained, leucocratic of buff, reddish brown and light grey colour and show the same textural features (flow and porphyritic). They are composed of phenocrysts (0.6–2.8 mm across) of plagioclase (An_{23-35}), potash feldspar and less frequent amphibole embedded in a fine grained flow banded groundmass consisted of the same minerals together with biotite and minor apatite and sphene. Amphibole forms subedral prismatic phenocrysts and as fine grains in the groundmass. Compositionally, the amphibole phenocrysts are sometimes zoned (*Fig. 4*), showing yellow to brown cores and brown to brownish green colour rims. On the other

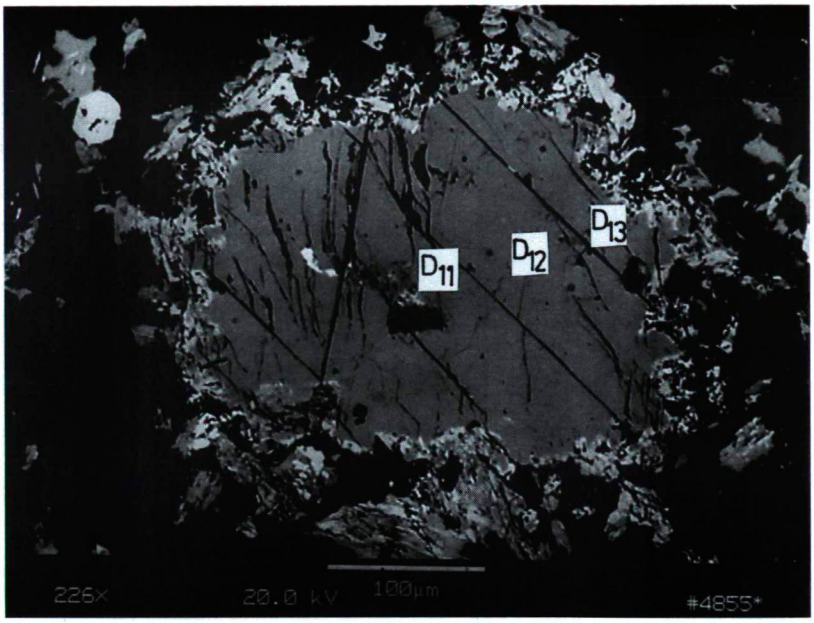

Fig. 3. Photomicrograph of a homogenous phenocryst from trachydacite-dacite (TD-D) suite showing ferroan pargasite composition, occasionally rimmed by a thick alteration margin consists of uralite, chlorite and Fe-oxide

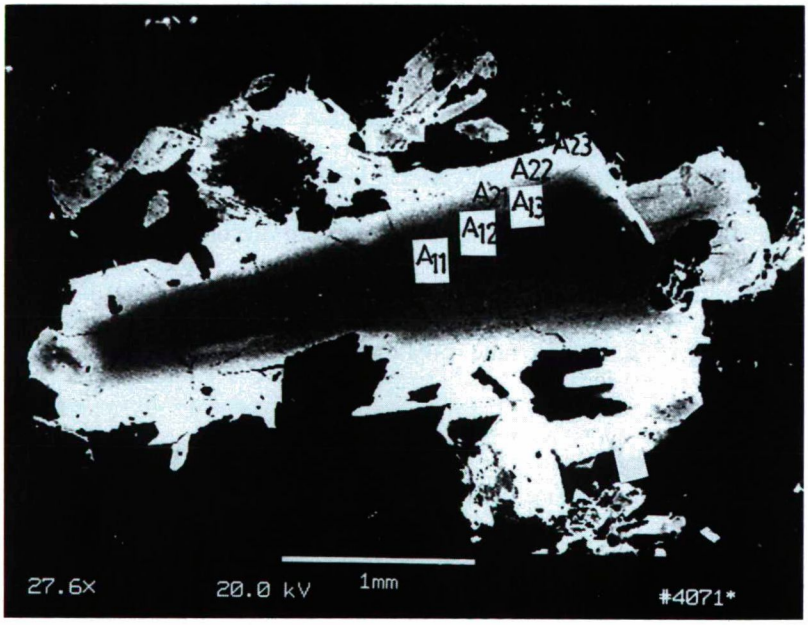

Fig. 4. Photomicrograph of a zoned phenocryst from rhyodacite-alkali rhyolite (RD-AR) suite showing kaersutite inner core, ferroan pargasite outer core and magnesian hastingsitic hornblende rim.

TABLE I

Representative whole-rock chemical compositions (wt. %) of the Kid volcanics

	Lower volcanic sequence		Middle volcanic sequence			
	Bas. andesite-andesite		Trachydacite-dacite		Rhyodacite-rhyolite	
	1	2	3	4	5	6
SiO_2	58.50	60.30	65.05	67.44	69.30	71.05
TiO_2	0.84	0.71	0.32	0.25	0.20	0.17
Al_2O_3	15.80	15.50	14.20	13.70	13.83	13.04
Fe_2O_3	1.20	1.04	1.15	1.02	0.73	0.65
FeO	5.23	4.98	2.70	2.40	2.10	2.05
MnO	0.06	0.07	0.04	0.04	0.04	0.03
CaO	4.95	4.80	1.98	1.75	1.78	1.65
MgO	2.54	2.22	1.20	0.93	1.10	1.04
Na_2O	4.25	4.37	4.45	4.55	4.66	4.73
K_2O	2.28	2.33	4.90	4.73	4.85	4.50
H_2O^-	0.54	0.48	0.72	0.61	0.19	0.20
P_2O_5	0.13	0.20	0.05	0.06	0.04	0.05
LOI	2.08	2.11	1.90	1.80	1.00	0.75
Sum.	99.12	99.09	98.66	99.28	99.82	99.91

hand, the grains of the groundmass are homogenous and show colours analogous to outer rims of the phenocrysts. A few amphibole grains are cracked and partially altered to chlorite and Fe-oxides or to biotite.

WHOLE ROCK CHEMISTRY

For the purpose of this study, it may useful to outline some chemical features and range of compositions of the amphibole host rocks to support field and mineralogical distinctions. Table 1 shows the results of the chemical analysis. A plot of the K_2O versus SiO_2 (*Fig. 5a*, PECCERILLO and TAYLOR, 1976) gives the best chemical classification of the studied volcanic sequences. Rocks represent the lower sequence fall into the andesite field, while those from the middle sequence correspond to trachyte, dacite and rhyolite. Most of these rocks belong to K-rich calc-alkaline series. A plot of (Na+K) versus Si (*Fig. 5b*) provides the best discriminant between the Kid volcanic sequences. Rocks of BA-A suite have low silica and alkalis and exhibit a positive trend. On the other hand, the TD-D and RD-AR suites have higher contents of silica and alkalis compared to the BA-A suite with a negative slope. The RD-AR suite contains the highest Si values.

ANALYTICAL TECHNIQUE

Mineral analyses were obtained using polished thin sections, which were vacuum-ccoated with carbon. A total of 30 amphibole analyses for the phenocrysts and groundmass of three samples representative the BA-A, TD-D and RD-AR suits of the Kid volcanics, were analyzed and given in Table 2. The analyses were carried out using the computerized Amray-1830 I electron microprobe under operating condition of 20kV and 1–2 nA. The structural formulae were calculated on the basis of 23 oxygens. In most cases, core and rim compositions were determined for zoned amphibole grains.

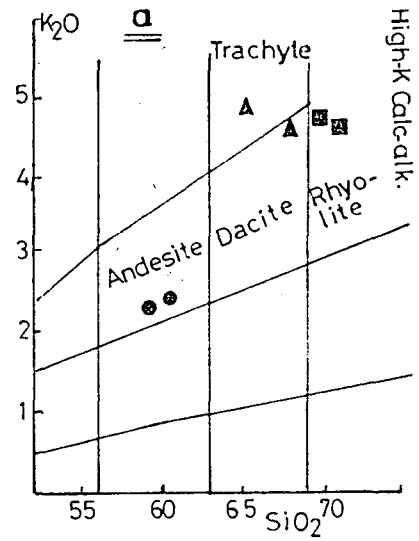

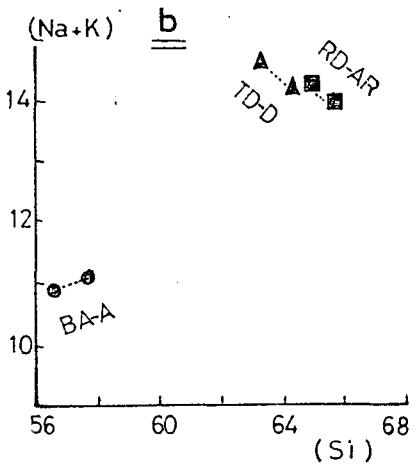

Fig. 5. Plots show the chemical characters of the whole rock samples from Kid volcanic suites.
A) K20 vs SiO_2 diagram after PECCERILLO and TAYLOR (1976). B) (Na+K) vs Si variation diagram (in cation percent).

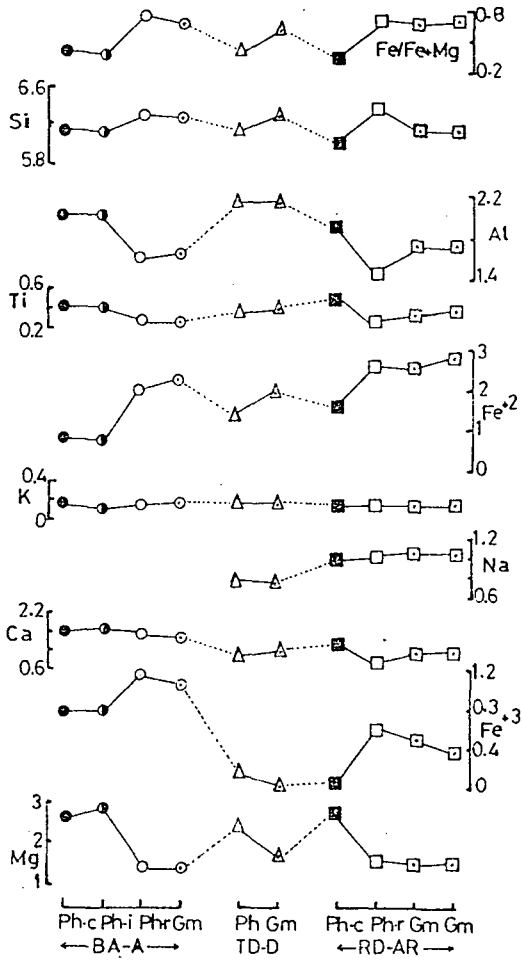

Fig. 6. Microprobe traverse through the amphibole phenocrysts (Ph) of *Fig. 2, 3 and 4* and groundmass (Gm) from Kid volcanic suites. The horizontal scale is arbitrary. Ph-c, -i, -r: present averages of phenocryst cores, intermediate portions and rims. Gm: averages of groundmass.

Chemical composition of amphiboles in the Kid volcanics

	Basaltic andesite-andesite (BA-A)												Trachydac-Dacite (TD-D)					
	Ph-c B-11	Ph-c B12	Ph-c B13	Ph-i B21	Ph-i B22	Ph-i B23	Ph-r B31	Ph-r B32	Ph-r B33	Gm-c A11	Gm-i A12	Gm-r A13	Ph-c D11	Ph-i D12	Ph-r D13	Gm-c F11	Gm-i F12	Gm-r F13
SiO_2	41.70	41.84	41.81	41.66	41.52	41.82	40.89	40.68	41.06	40.85	40.90	40.93	41.80	41.55	41.29	41.95	41.53	41.75
TiO_2	4.13	4.21	4.03	4.03	3.94	4.04	2.77	2.71	2.56	2.75	2.72	2.76	3.84	3.81	3.83	3.94	3.87	3.90
Al_2O_3	11.61	11.92	11.65	11.67	11.70	11.96	8.60	8.25	8.60	8.70	8.65	8.75	12.70	12.91	13.04	11.98	12.21	12.50
FeO_t	13.59	13.75	13.42	12.84	12.89	12.72	27.70	27.61	27.39	27.80	27.05	27.25	13.10	13.35	13.40	15.32	15.75	15.80
MnO	–	–	–	–	–	–	–	–	–	–	–	–	–	–	–	–	–	–
CaO	12.66	12.60	12.56	12.68	12.55	12.84	11.01	11.31	11.25	11.32	11.25	11.50	11.23	11.33	11.40	11.20	11.12	11.35
MgO	12.46	12.58	12.90	12.96	13.12	12.97	5.65	5.52	6.11	5.72	5.78	5.83	12.11	11.44	11.46	7.55	7.35	7.58
Na_2O	–	–	–	–	–	–	–	–	–	–	–	–	–	–	–	–	–	–
K_2O	0.70	0.89	0.62	0.60	0.63	0.69	0.99	0.92	0.90	0.95	0.92	0.97	0.84	0.77	0.80	0.93	0.94	0.90
Cr_2O_3	–	–	–	–	–	–	–	–	–	–	–	–	–	–	–	–	–	–
Sum	96.85	97.79	96.99	96.44	96.35	97.04	97.61	97.00	97.87	98.56	98.12	98.64	98.21	97.74	97.98	95.62	95.65	96.71
Si	6.131	6.091	6.106	6.120	6.092	6.114	6.276	6.314	6.270	6.252	6.301	6.275	6.129	6.149	6.112	6.417	6.372	6.336
Al_4	1.869	1.909	1.894	1.880	1.908	1.886	1.556	1.509	1.548	1.569	1.471	1.581	1.871	1.851	1.888	1.583	1.628	1.664
Fe^{3+}	0.000	0.000	0.000	0.000	0.000	0.000	0.168	0.177	0.182	0.179	0.128	0.144	–	–	–	–	–	–
Sum	8.000	8.000	8.000	8.000	8.000	8.000	8.000	8.000	8.000	8.000	8.000	8.000	8.000	8.000	8.000	8.000	8.000	8.000
Al_6	0.143	0.136	0.111	0.140	0.115	0.175	0.000	0.000	0.000	0.000	0.000	0.000	0.324	0.401	0.387	0.577	0.580	0.572
Cr	–	–	–	–	–	–	–	–	–	–	–	–	–	–	–	–	–	–
Ti	0.457	0.461	0.443	0.445	0.435	0.444	0.320	0.316	0.294	0.316	0.315	0.318	0.423	0.424	0.426	0.435	0.447	0.445
Fe^{3+}	0.684	0.744	0.837	0.734	0.845	0.663	1.224	1.074	1.239	0.946	0.895	0.832	0.277	0.124	0.090	–	–	–
Mg	2.730	2.730	2.808	2.838	2.869	2.826	1.293	1.277	1.391	1.315	1.327	1.332	2.647	2.523	2.528	1.721	1.681	1.715
Fe^{2+}	0.986	0.929	0.801	0.843	0.736	1.892	2.163	2.333	2.076	2.433	2.462	2.518	1.329	1.528	1.569	1.964	2.021	2.005
Mn	–	–	–	–	–	–	–	–	–	–	–	–	–	–	–	–	–	–
Sum	5.000	5.000	5.000	5.000	5.000	5.000	5.000	5.000	5.000	5.000	4.999	5.000	5.000	5.000	5.000	4.715	4.730	4.737
Fe^{2+}	0.001	0.001	0.001	0.000	0.001	0.001	0.000	0.000	0.001	–	–	–	–	–	–	–	–	–
Ca	1.994	1.965	1.965	1.996	1.973	2.011	1.811	1.881	1.841	1.856	1.857	1.889	1.764	1.796	1.808	1.836	1.828	1.846
Na	–	–	–	–	–	–	–	–	–	0.144	0.143	0.111	0.236	0.204	0.192	0.164	0.172	0.154
Sum	1.995	1.966	1.966	1.996	1.974	2.012	1.811	1.881	1.841	1.856	1.857	1.889	1.764	1.796	1.808	1.836	1.828	1.846
Na	–	–	–	–	–	–	–	–	–	0.099	0.111	0.157	0.500	0.536	0.600	0.652	0.685	0.708
K	0.131	0.165	0.115	0.112	0.118	0.129	0.194	0.182	0.175	0.185	0.181	0.190	0.157	0.145	0.151	0.181	0.184	0.174
total	15.13	15.13	15.08	15.11	15.09	15.14	15.00	15.06	15.02	15.28	15.29	15.35	15.66	15.68	15.75	15.55	15.60	15.62

Ph = phenocrysts, Gm = groundmass, c = core, i = intermediate portion, r = rim, All = number of analysis.

TABLE 2 contd.

	Rhyodacite-rhyolite (RD-AR)											
	Ph-c A11	Ph-c A12	Ph-c A13	Ph-c A21	Ph-c A22	Ph-c A23	Gm-c C11	Gm-i C12	Gm-r C13	Gm-c E11	Gm-i E12	Gm-r. E13
SiO_2	40.26	40.68	40.42	41.56	41.23	41.75	39.49	39.55	39.22	38.60	39.10	39.14
TiO_2	4.52	4.15	4.32	2.15	2.20	2.08	2.76	2.86	2.87	3.27	3.12	3.22
Al_2O_3	10.83	10.87	10.96	7.36	7.41	7.51	9.14	8.84	9.30	9.32	9.17	9.23
FeO_t	12.93	12.89	12.60	25.99	25.96	25.75	24.03	24.44	24.11	23.40	24.12	24.14
MnO	0.00	0.00	0.00	0.35	0.35	0.40	0.36	0.41	0.35	0.32	0.28	0.21
CaO	11.84	12.08	12.06	10.34	10.37	10.49	10.65	10.77	10.59	10.71	10.80	10.63
MgO	12.73	12.63	12.60	6.69	6.58	6.78	6.96	7.00	6.97	6.80	6.85	6.42
Na_2O	3.33	3.17	3.64	3.31	3.40	3.58	3.66	3.53	3.63	3.87	3.44	3.58
K_2O	0.68	0.67	0.68	0.86	0.83	0.80	0.82	0.82	0.80	0.86	0.85	0.81
Cr_2O_3	0.29	0.28	0.25	0.00	0.00	0.00	0.00	0.00	0.00	0.00	0.00	0.00
Sum	97.41	97.42	97.35	98.61	98.33	99.14	97.87	98.22	97.84	97.15	97.73	97.38
Si	6.054	6.107	6.068	6.443	6.424	6.450	6.177	6.169	6.129	6.118	6.134	6.177
Al_4	1.919	1.893	1.932	1.345	1.361	1.367	1.685	1.625	1.713	1.741	1.695	1.717
Fe^{3+}	0.000	0.000	0.000	0.212	0.215	0.183	0.188	0.206	0.158	0.141	0.171	0.106
Sum	8.000	8.000	8.000	8.000	8.000	8.000	8.000	8.000	8.000	8.000	8.000	8.000
Al_6	0.000	0.030	0.007	0.000	0.000	0.000	0.000	0.000	0.000	0.000	0.000	0.000
Cr	0.034	0.033	0.030	–	–	–	–	–	–	–	–	–
Ti	0.511	0.469	0.488	0.251	0.258	0.242	0.325	0.335	0.337	0.390	0.368	0.382
Fe^{3+}	0.000	0.000	0.000	0.446	0.397	0.356	0.326	0.322	0.384	0.100	0.279	0.204
Mg	2.853	2.826	2.819	1.546	1.528	1.561	1.623	1.628	1.624	1.606	1.602	1.510
Fe^{2+}	1.626	1.618	1.582	2.712	2.772	2.788	2.679	2.660	2.609	2.860	2.714	2.876
Mn	0.000	0.000	0.000	0.046	0.046	0.052	0.048	0.054	0.046	0.043	0.037	0.028
Sum	4.997	4.976	4.926	5.000	5.000	4.999	5.000	4.999	5.000	4.999	5.000	5.000
Fe^{2+}	–	–	–	–	–	–	–	–	–	–	–	–
Ca	1.908	1.943	1.940	1.718	1.731	1.736	1.785	1.800	1.773	1.819	1.815	1.797
Na	0.092	0.057	0.060	0.281	0.269	0.264	0.214	0.200	0.227	0.181	0.185	0.203
Sum	2.000	2.000	2.000	2.000	2.000	2.000	2.000	2.000	2.000	2.000	2.000	2.000
Na	0.879	0.866	0.999	0.714	0.758	0.808	0.896	0.868	0.873	1.008	0.861	0.892
K	0.130	0.128	0.130	0.170	0.165	0.158	0.164	0.164	0.159	0.174	0.170	0.163
total	16.00	15.97	16.05	15.88	15.92	15.97	16.06	16.03	16.03	16.18	16.03	16.05

AMPHIBOLE CHEMISTRY

Microprobe analytical results of the amphiboles from the Kid volcanics, along with the calculated number of ions per unit cell, are reported in Table 2. All the amphibole compositions from the different sequences of the Kid volcanics are, in general, characterized by $(Ca+Na)_B$ > or = 1.34 and Na_B < 0.67 (i. e., calcic-type amphibole), and rich in Ca, Mg and Al. Moreover, the present amphibole is characterized by their high Ti contents (Ti = 0.24–0.51) (Table 2) probably reflect their derivation from Ti-rich pyroxene.

The analyzed calcic amphiboles of various volcanic suites are exhibited wide compositional variations (*Fig. 6*) and classified according to the IMA classification (LEAKE, 1978, *Fig. 7*).

The analyzed amphiboles of the basaltic andesite-andesite (BA-A) suite of the lower sequence comprise phenocrysts and groundmass. The phenocrysts exhibit normal zoning towards Fe-K-Si-rich and Mg-Ti-poor rims (*Fig. 6*). Both the inner and outer parts of the phenocryst cores (i. e., Ph-c and Ph-i; *Fig. 6*) are generally similar in composition, but the outer core is richer in Mg and Ca contents. Phenocrysts of the BA-A suite are tschermakite cores and ferro tschermakitic hornblende rims (*Fig. 7a*). In this case, significant substitution of Fe^{3+} of ferro tschermakitic hornblende for Al, i. e. $[Al^6]$ of tschermakite, can occur. The present phenocrysts contain the highest values of Fe^{3+}/Fe^{2+} ratio among the Kid volcanics, which are probably the result of highly oxidizing conditions that may have dominated, locally during the hydrothermal stage at relatively lower temperature. The groundmass amphiboles and the outermost rims of phenocrysts are commonly analogous, but with a less Fe^{3+}/Fe^{2+} ratio, probably corresponded to the decrease of oxidizing process as well as the differences in their condition of crystallization. The groundmass amphiboles are homogenous, showing ferro tschermakitic hornblende (*Fig. 7a*).

The analyzed amphiboles of the Trachydacite-dacite (TD-D) suite of lower unit of the middle sequence are compositonally homogeneous. The phenocrysts are ferroan pargasite, whereas the groundmass amphiboles are ferroan pargasitic hornblende (*Fig. 7b*). Amphibole phenocrysts from TD-D suite tend to be poorer in Mg and Ca and richer in Fe^{2+}, K and Na than are those from BA-A suite, suggesting a progressive magmatic evolution. Furthermore, Fe^{2+}, Si and K increase and Mg decreases from phenocrysts toward the groundmass (*Fig. 6*), indicating a more evolutionary groundmass amphiboles. Moreover, the ferroan pargasite phenocryst contains contents of Fe^{3+}, probably indicate an oxidizing condition probably during hydrothermal stage. Conversely, the ferroan pargasitic hornblende groundmass is free from Fe^{3+}.

The analyzed amphiboles of the rhyodacite-alkali rhyolite (RD-AR) of upper unit of the middle sequence represent the phenocrysts and groundmass. The phenocrysts exhibit normal zoning showing a wide range of composition towards Fe-, Mn-, Na- and Si-rich and Cr-Mg-poor rims (*Fig 6*; Table 2). The amphibole phenocrysts from RD-AR suite tend to have the same trends of the BA-A suite but poorer in Al and Fe^{3+} and more rich in Fe^{2+} (*Fig. 6*) probably suggest cognate magma. The cores of phenocrysts consist of kaersutite inner part (*Fig. 7c*) and ferroan pargasite outer part (*Fig. 7b*), whereas the rims are magnesian hastingsitic hornblende (*Fig. 7c*). Kaersutite is Ti-rich (Ti > 0.5) version of pargasite. In this case, substitution of Fe^{3+} of the magnesian hastingsitic hornblende rims for Al^6 of the ferroan pargasite cores, can occur. These cores (i. e., kaersutite and ferroan pargasite) contain Mn. Furthermore, these phenocryst cores are similar to the phenocryst of the TD-D suite (i. e., ferroan pargasite). The groundmass amphiboles, on the other hand, are magnesian hastingsites (*Fig. 7d*), and are nearly equivalent to the phenocryst

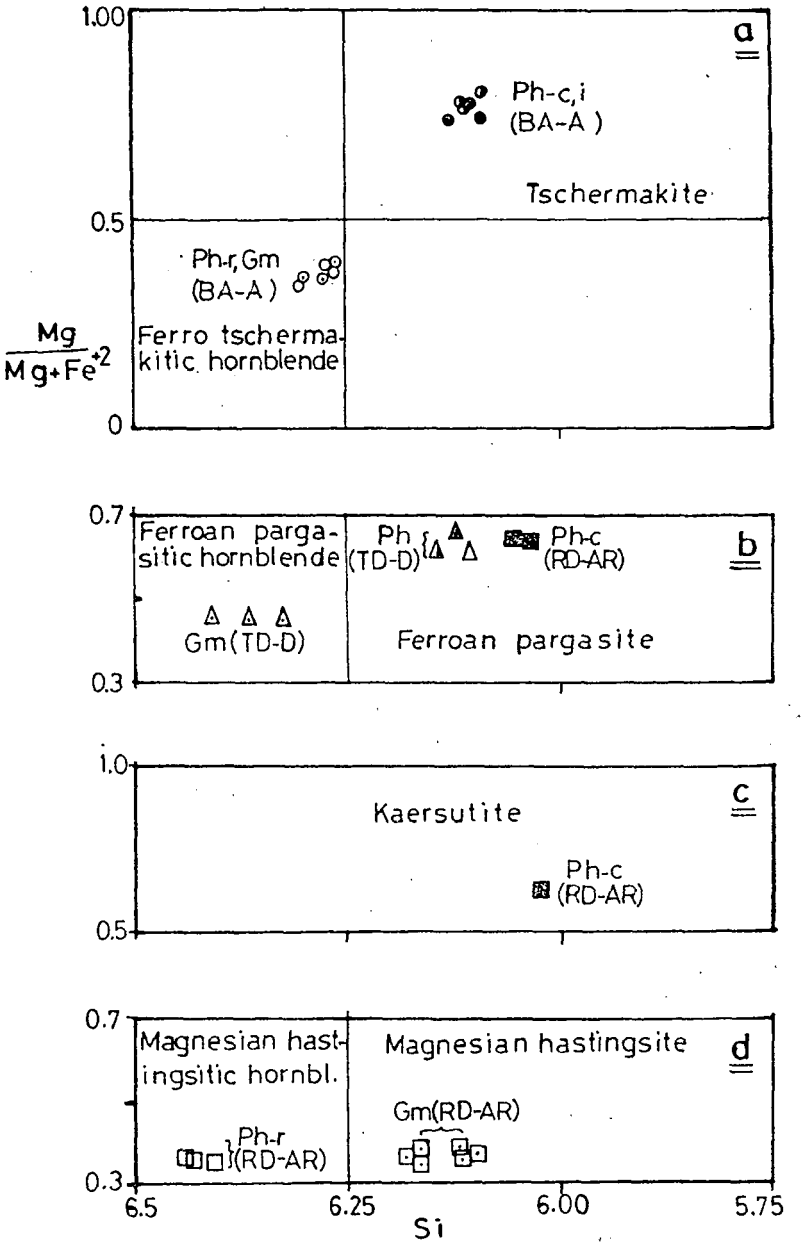

Fig. 7. Classification of calcic amphiboles (LEAKE, 1978) of Kid volcanic suites.
a) $(Na+K)_A < 0.5$; $Ti < 0.5$; b) $(Na+K)_A \geq 0.5$, $Ti < 0.5$, $Fe^{3+} \leq Al6$; c) $Ti \geq 0.5$; d) $(Na+K)A \geq 0.5$, $Ti < 0.5$, Fe3+ > Al6. BA-A = Basaltic andesite-andesite, TD-D = trachydacite-dacite, RD-AR = rhyodacite-alkali rhyolite. Symbols as in *Fig. 6*.

rims, with less Si and Ti and more Mg. The magnesian hastingsites are equivalent to Fe^{3+} rich ferroan pargasites (Fe^{3+} > $[Al^{6}]$). The entry of Fe^{3+} into hornblende can also be balanced by the substitution of O for [OH] (DEER et al., 1992). The amphibole groundmass form RD-AR suite tend to be lowest in Ti and Ca and highest in Na, Mn and Fe/(Fe+Mg) ratio among the other amphibole groundmasses of the Kid volcanics (*Fig. 6*), suggesting that they are the highest differentiated volcanic phase.

DISCUSSION

The data presented here allow some interpretations to be made concerning: a) the tschermakite-kaersutite-ferroan pargasite-magnesian hastingsite end-member relationships, b) evolutionary trends for amphiboles, c) metamorphism and geobarometer, d) implications for magma evolution.

The tschermakite-pargasite-hastingsite relationships

These relationships have been studied by several investigators, including HAWTHORNE (1983), HAMMARSTROM and ZEN (1986), FLEET et al. (1987), BEDARD (1988), HENDERSON et al. (1989), SCHULZ-KUHNT et al. (1990) and DEER et al. (1992). Oxy-hornblendes have a wide range of compositions which constitute the main calcic amphiboles in volcanic rocks. In this case, the iron-rich version usually with $Fe^{2+}/(Fe^{2+}+Mg) > 0.5$ can be indicated by the prefix „ferro". Within the calcic-amphiboles, as a whole the range of Fe/(Fe+Mg) ratio is complete but those with high Si content tend to be more „Mg-rich", whereas among tschermakitic and pargasitic hornblende, iron-rich members are more common. In the more iron-rich hornblendes, the Fe^{3+}-rich equivalents (Fe^{3+} > $[Al]^{6}$) of pargasite and ferroan pargasite are respectively called magnesian hastingsite. Ti-rich (Ti>0.5 atom) version of pargasite is kaersutite (DEER et al., 1992).

Kaersutite has a formula similar to that of pargasite, but Ti replaces Al in C-sites. Kaersutite, like oxyhornblende, it mostly Mg-rich with substitution of Mg by (Fe^{2+}+Fe^{3+}). Kaersutite can be oxidized during eruption, converting Fe^{2+} to Fe^{3+} and OH to O. It is a typical constituent of alkaline volcanic rocks, occurs as phenocrysts and can be replaced Ti-augite (DEER et al., 1992). Hastingsite (usually primary hornblende) occurs in the rocks of the calc-alkaline series, where the f_{H_2O} and f_{O_2} are high. The typical hastingsite of the intermediate rocks of the calc-alkaline series have Mg/(Mg+Fe) ratio ~0.5 and a moderate content of Al (~1.5). The hastingsite of andesitic rocks tend to richer in alkalis and Fe^{3+} (DEER et al., 1992).

The amphibole of Kid volcanics is characterized by compositional changes, i. e. tschermakite → Fe-tschermakitic hornblende in BA-A suite, Fe-pargasite → Fe-pargasitic hornblende in TD-D suite and Kaersuite → Fe-pargasite → Mg-hastingsitic hornblende in RD-AR suite. The overall compositional change of the Kid hornblende is characterized by the change of tschermakite → pargasite and hastingsite.

Evolutionary trend of the amphibole

Amphiboles of Kid volcanics have a wide range of compositions. *Fig. 8* displays the major element chemical variation as a function of the evolution index Fe/(Fe+Mg). The Fe/(Fe+Mg) ratio varies from 0.36–0.74 and a trend of increasing Si+Na+K, corresponding to a decrease in Ca+Al4 from phenocryst cores to phenocryst rims and

groundmass (*Fig. 9a*), is apparent as the amphiboles become more Fe-rich. The evolution index [Fe/(Fe+Mg) ratio] of the amphibole phenocrysts increases from cores (0.36–0.38) towards the rims (0.40–0.74). However, the cores of phenocrysts of BA-A, TD-D and RD-AR suites have similar values of Fe/(Fe+Mg) raito and Ca+Al4 (*Fig. 8., 9a*), suggesting a cognate magma for these suites. This ratio ranges from 0.53–0.68 in the groundmass of these suites, which are indistinguishable from the rims of phenocrysts. The evolution of these amphiboles was mainly controlled by the Fe ↔ Mg and Al6 ↔ Fe3+ substitution schemes.

The amphiboles of Kid volcanics range from tschemakite and ferroan tschermakitic hornblende in the BA-A suite, through ferroan pargasite and ferroan pargasitic hornblende in T-D suite to kaersutite, ferroan pargasite, magnesian hastingsitic hornblende and magnesian hastingsite in the RD-R suite (Table 2). The evolutionary trend is characterized by decreasing Ca, Mg, Cr, Fe^{3+} and Al, increasing Na and Fe^{2+}, and almost constant K, Ti and Si (*Fig. 6*). The variations in amphiboles (i. e., from BA-A suite of the lower sequence to RD-AR suite in the upper unit of the middle sequence) are responsible for the magmatic evolution of the Kid volcanics. Furthermore, the decrease in $Ca+Al_4$ and increase in Si+Na+K are gradually increased from BA-A suite of the lower sequencesuite to RD-D and RD-AR suite of the middle sequence (*Fig. 9a*), indicating again the progressive fractionation trend of the amphiboles. On the other hand, ferric-ferrous (Fe^{3+}/Fe^{2+}) ratio in these amphiboles is gradually decreased in the same direction. This suggest a gradual decrease in f_{O_2} (i. e., the melt becomes less oxidized) with differentiation of the volcanic suites.

The data presented show that there is only a calcic-type trend of the amphibole. This is probably due to the stability of the early formed Ca-rich amphibole phenocrysts, with the progressive increase in the alkalinity of the melt. Consequently, the absence of a gap miscibility in this amphibole. However, a probable small gap may be existed between amphiboles of lower and middle volcanic sequence.

Amphibole Metamorphism and Geobarometer

Hornblende is one of the most common constituens of regionally metamorphosed basic-intermediate rocks and is stable under a wide range of pressure-temperature conditions. The amphibole assemblage of the Kid volcanics as well as the probable metamorphic facies are summarized (Table 3). Both of BA-A and TD-D suites are overprinted by upper epidote amphibolite and lower amphibolite facies, whereas the RD-AR suite shows mineral assemblage similar to the upper greenschist and lower epidote amphibolite facies. Increasing grade of metamorphism tends to produce changes in amphibole composition, i. e. increases in Al, Ti, Na and K, but rock composition and oxygen fugacity are influential as well as temperature (DEER et al., 1992).

HAMMARSTROM and ZEN (1986) reported the compositional dependence of amphibole on temperature (T), pressure (P), oxygen fugacity (f_{O_2}) and bulk composition. T tends to increase with increasing Al^4, Ti, and $Mg/(Mg+Fe^{2+})$ ratio and decreasing Al^{6+}, Mn and $Fe^{3+}/(Fe^{3+}+Fe^{2+})$ ratio. P increases with increasing Al^6 and Al^T. F_{O_2} appears to increase with increasing Al^T and $Mg/(Mg+Fe^{2+})$ ratio and decreasing Ti. The bulk composition usually increases with increasing concentration of Si, Ti, alkalis and $Mg/(Mg+Fe^{2+})$ ratio in the system.

In the Kid volcanics, the amphibole phenocrysts of both BA-A and RD-AR suites are characterized by decrease in Ti, Al^4 and $Mg/(Mg+Fe^{2+})$ ratio from cores to rims (*Fig. 8, 9a and 9b*), suggest a decrease in T of crystallization toward the phenocryst rims. Also,

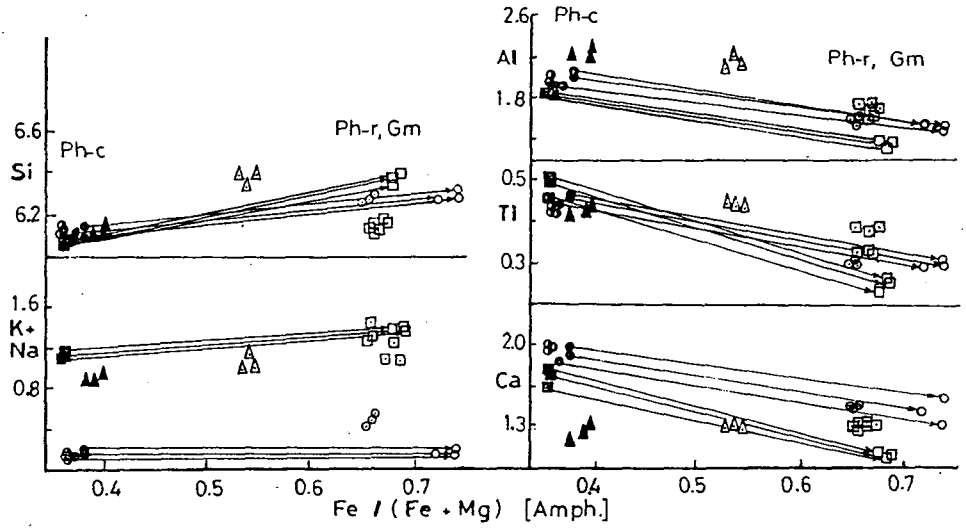

Fig. 8. Variation of Si, K+Na, Al, Ti and Ca versus Fe/(Fe+Mg) ratio of the amphiboles from Kid volcanics. The tie lines join the phenocryst cores and phenocryst rims. Symbols as in *Fig. 6.*

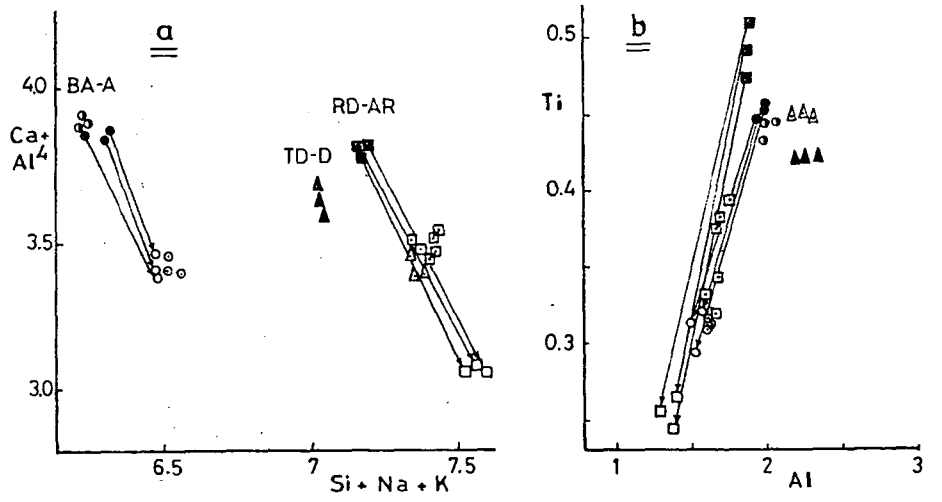

Fig. 9. Plots show the compositional variations of the phenocryst cores and rims and groundmass of the amphiboles of Kid volcanics.
a) (Ca+Al4) vs. (Si+Na+K) diagram. b) Ti vs. Al diagram. Symbols as in *Fig. 6.*

P appears to be decreased with decreasing Al^6 and Al^T. F_{O_2} tends to increase with decreasing Ti from cores to rims of phenocrysts. Furthermore, metamorphic grade of these rocks decrease with decreasing Al^T, Ti and alkalis from BA-A suite of the lower sequence to RD-AR suite of the middle volcanic sequnce and from cores to rims of phenocrysts, revealing that the early formed stage (e. g., BA-A suite) is more affected by metamorphism than the latter. These features are consistent with the higher metamorphic grade of the Old Dokhan volcanics or the lower volcanic sequence (e. g., BA-A suite) reported by EL-GABY et al. (1991) and HASSANEN (1992).

Implications for magma evolution

Petrographic studies (e. g., *Fig. 2, 3 and 4*) combined with the microprobe analytical data presented, have decumented the presence of compositional normal zoning in the amphibole grains. The dominant substitution mechanisms in amphiboles from mafic to intermediate silica-saturated and oversaturated alkaline rocks are thought to be (Na, K)^{A}Al^4 ↔ [ ]^{A}Si, Ca(Mg, Fe^{2+}) ↔ Na^MFe^{3+vi} and Mg = Fe^{2+} (NEUMANN, 1976; GIRET et al., 1980; STEPHENSON and UPTON, 1982).

Amphibole phenocrysts. Amphibole phenocrysts from the basaltic andesite-andesite (BA-A) suite range from tschermakite core to ferro tschermakitic hornblende rims and display a strongly increase in Si, Fe and K and decrease in Al, Mg, Ca and Ti toward the rims (*Fig. 6, 8 and 9a*), together with decrease Fe^{3+}/Fe^{2+} ratio (average of 0.84 core – 0.61 rim), suggests that the BA-A suite of the lower sequence has evolved from an early (subalkaline) melt that started its crystallization under oxidizing conditions. However, these compositional relations are believed to represent normal magmatic zoning. The substitution mechanisms in amphiboles of the BA-A suite are thought to be $[Al]^6$ ↔ Fe^{3+}, Mg ↔ Fe and Ca+Al ↔ Na+Si.

TABLE 3

Amphibole mineral assemblages in Kid volcanic complex

Mineral assemblage	Suite	Greenschist facies	Epidote amphibolite facies		Amphibolite facies
		A2	B1	B2	C1
Tschermakite	BA-A				----------
Tsch. hornbl.	BA-A			----------	----------
Pargasite	TD-D			----------	----------
Parg. hornbl.	TD-D			----------	
Kaersutite	RD-AR			----------	----------
Hastingsite	RD-AR	----------	----------		
Hast. hornbl.	RD-AR	----------	----------		

Amphibole phenocrysts from rhyodacite-alkali rhyolite (RD-AR) suite in the lower unit of the middle sequence range from kaersutite and ferroan pargasite core to magnesian hastingsitic hornblende rims, displaying compositional trends analogue to that from BA-A suite above (e. g., strongly increase of Si, Fe, K, Na and Mn and decrease of Al, Ti, Mg, Cr and Ca toward the rims (*Fig. 6, 8 and 9a*), suggests the genetic links of their parental magma. Furthermore, the compositional trend of the RD-AR suite may reflect a progressive fractionated magma. The substitution mechanisms in these amphiboles are

thought to be $Ti+O \leftrightarrow Fe^{3+}+OH^-$. The RD-AR suite magma probably had low silica activities. This would inhibit substitution such as $CaAl^4 \leftrightarrow Na^MSi$ and should result in a limited range of $Ca+Al^4$ vs. Si+Na+K variation, as is observed. RD-AR suite amphiboles show limited Na-enrichment and Ca-depletion. This implies that the substitutions like Ca (Mg, Fe^{2+}) Na^MFe^{3+vi} did not occur to great extent. Both the TD-D and RD-AR suites of the middle sequence are characterized by a quite similarity in composition and evolution, suggest a genetic relationship of their cognate magma.

Amphibole groundmass. Amphibole groundmass from BA-A suite is ferro tschermakitic hornblende which is quite similar to the phenocryst rims of the same rocks. Groundmass and phenocryst amphiboles from TD-D suite are also analogous. However, groundmass amphiboles are slightly enriched in Si and Fe^{2+} and depleted in Mg and Fe^{3+}, probably reflect their fractionation. On the other hand, the groundmass amphiboles from RD-AR suite are magnesian hastingsites and tend to be depleted in Cr, Fe^{3+} and $Ca+Al^4$ and enriched in Fe^{2+} and Na compared with the phenocryst rims of the same rocks reflecting their intermediate crystallization between the phenocryst cores and rims.

Although the stability of tschermakite at high-P conditions has been studied (e. g., GILBERT et al, 1981), its thermal stability at low-P conditions has yet to be defined. However, results of experimental studies applied to phase equilibrium of tremolite, which is similar to tschermakite, is available. BOYD (1969) has studied the P-T stability of tremolite. On his phase diagram, tremolite (as well as tschermakite-tschemakitic hornblende of BA-A suite) appears in a field, between T of ~ 800 °C and 900 °C at P of 0.5–3 Kbar. On the other hand, HANDERSON et al. (1989) have established, by means of amphibole composition, that the range of T of crystallization is 950–1000 °C for kaersutite and 750–800 °C for hastingsite. The stability limits of the pargasite. Fe-pargasite, Mg-hastingsite and hastingsite as a function of T and P have been studied by GILBERT et al. (1981). On the T side of his phase diagram, Fe-pargasite has maximum stability at f_{O_2} of the wustite-magnetite buffer (e. g., T: < 700–870 °C and P: 0.5–2.2 Kb.), whereas the more Fe^{3+}-rich Mg hastingsite has maximum stability with the hematite-magnetite buffer (e. g., T: 900–1030 °C and P: 0.2–0.6 Kb). These results seem to be concordant with the decrease of T and P as well as the metamorphic grade from BA-A suite of the lower sequence to RD-AR suite of the middle sequence (e. g., from cores to rims of phenocrysts and groundmass).

It is common to see a sharp optical and compositional boundary (*Fig. 2, 3, 4, 8 and 9a*) between the core and rims of the phenocrysts. The sharp discontinuity suggests a sudden transition from one growth environment to another and may reflect rapid ascent or sudden change in equilibrium caused by volatile exsolution (BEDARD, 1988) in the Ca-amphibole group itself.

In summary, the role of amphibole during magmatic differentiation may control the composition of the derivative melt. For example, the $Mg \leftrightarrow Fe$, $CaFe^{2+} \leftrightarrow NaFe^{3+}$ and $CaAl \leftrightarrow NaSi$ substitution mechanisms in the Ca-amphiboles of the Kid volcanics, have led to magma evolution from intermediate to felsic compositions (e. g. from BA-A suite of the lower seuence to TD-D and RD-AR suite of the middle volcanic sequence). The phenocrysts of both BA-A nd RD-AR suites show a same compositional trend; this implies that they are cognate with higher temperature and f_{O_2} and lower pressure cores than the rims. Amphiboles that characterize these suites (e. g., tschermakite, kaersutite, Fe-pargasite and Mg-hastingsite) are breakdown to form discontinuous zoned, calcic-type amphibole with a progressive increase in the alkalinity, silica and iron of the melt. These amphiboles are expected to be formed at high temperature (~700-1000 °C) and low pressure (~0.2-3 Kb.).

REFERENCES

BEDARD, J. H. (1988): Comparative amphibole chemistry of the Moteregian and White Mountain alkaline suites, and the origin of amphibole megacrysts in alkaline basalts and lamprophyres. Min. Mag., **52**, 91–103.

BOYD, F. R. (1959): Hydrothermal investigations of the amphiboles. In: Research Geochemistry, P. H. Ableson (ed.), 377–396.

CAMERON, M., J. J. PAPIKE (1979): Amphibole crystal chemistry: a review. Fortschr. Miner., **57**, 28–67.

DEER, W. A., R. A. HOWIE, J. ZUSSMAN (1992): An introduction to the rock-forming minerals. Long. Sci. & Tech., England.

EL-GABY, S., A. A. KHUDEIR, M. ABDEL-TAWAB, R. F. ATALLA (1991): The metamorphosed volcano-sedimentary succession of Wadi Kid, Southeastern Sinai, Egypt. Annals Geol. Surv. Egypt, XVII, 19–35.

EL-GABY, S., F. K. LIST, R. TEHRANI (1988): Geology, evolytion and metallogenesis of the Pan-African belt in Egypt. The Pan-African belt of Northeastern Africa and adiacent countries. In: S. EL-GABY and R. GREILING (eds.). 17–68.

FLEET, M. F., R. L. BARNETT, W. M. MORRIS (1987): Prograde metamorphism of the Sudbury igneous complex. Can. Mineral., **25**, 499–514.

GHONEIM, M. F., S. M. ALY, M. H. EL-BARAGA (1985): Geochemistry of the Malhag metavolcanics, South Sinai Peninsula, Egypt. Annals Geol. Surv. Egypt., XV, 171–182.

GILBERT, M. C., R. T. HELZ, R. K. POPP, F. S. SPEAR (1981): Experimental studies of amphibole stability. Mineral. Soc. Amer., Rev. Mineral., **9B**, 279–353.

GIRET, A., B. BONIN, J.-M. LEGER (1980): Amphibole compositional tennds in oversaturated and under-saturated alkaline plutonic ring complexes. Can. Mineral., **18**, 481–495.

HASSANEN, M. H. (1992): Geochemistry and petrogenesis of the late Precambrian Kid volcanis: evidence relevant to arc-intra-arc rifting volcanism in Southern Sinai, Egypt. J. Afr. Earth Sci., **14**, 131–145.

HAMMARSTROM, J. M., E-AN ZEN (1986): Aluminium in hornblende: An empirical igneous geobarometer. Amer. Mineral., **71**, 1297–1313.

HENDERSON, C. M. B., K. PENDLENURY, K. F. FOLAND (1989): Mineralogy and petrology of the Red Hill alkaline igneous complex. New Ampshire, U. S. A. J. Petrol., **30**, 627–666.

HOWTHORNE, F. C. (1983): The crystal chemistry of amphiboles. Can. Mineral., **21**, 173–480.

LEAKE, B. E. (1978): Nomenclature of amphiboles. Can. Mineral., **16**, 501–520.

NEUMANN, E.-R. (1976): Two refinaments for the calculation of structural formulae for pyroxenes and amphiboles. Norsk Geol. Tidsske., **56**, 1–6.

PECCERILLO, A., S. R. TAYLOR (1976): Geochemistry of Eocene calc-alkaline volcanic rocks from Kastamonu area, northern Turkey. Contrib. Min. Petrol. , **58**, 63–81.

REYMER, A. P. S., A. MATHEWS, O. NAVON (1984): Pressure-temperature conditions in the Wadi Kid metamorphic complex: Implications for the Pan-African event in the southeastern Sinai. Contrib. Mineral. Petrol., **85**, 336–345.

RIES, A. C., R. M. SCHACKLETON, R. H. GRAHAM, W. R. FITCHES (1983): Pan-African structures, ophiolites and melanges in the Eastern Desert of Egypt: A traverse at 26 N. J. Geol. Soc. London, **140**, 75–95.

SCHULZ-KUHNT, D., G. MULLER, J. HOEFS (1990): Petrology of high-grade metamorphic terrains in the Abre Campo-Jequeri Quadrangle, Eastern Minas Gerais, Brazil. Chem. Erde, **50**, 225–245.

SHIMRON, A. E. (1984): Evolution of the Kid Group, Southeast Sinai Peninsula. Thrusts, Melanges and implications for accretionary tectonics during the late Proterozoic of the Arabian-Nubian Shield. Geology, **12**, 242–247.

Manuscript received 22 August 1995.